Transformation of Gels via Catalyst-Free Selective RAFT Photoactivation

Journal:	*Polymer Chemistry*
Manuscript ID	PY-ART-02-2019-000213.R1
Article Type:	Paper
Date Submitted by the Author:	05-Apr-2019
Complete List of Authors:	Shanmugam, Sivaprakash; UNSW Australia, Centre for Advanced Macromolecular Design (CAMD) Cuthbert, Julia ; Carnegie Mellon University, Department of Chemistry Flum, Jacob ; Carnegie Mellon University, Department of Chemistry Fantin, Marco; Carnegie Mellon University, Department of Chemistry Boyer, Cyrille; University of New South Wales, Centre Advances MAcromolecular Design Kowalewski, Tomasz; Carnegie Mellon University, Department of Chemistry Matyjaszewski, Krzysztof; Carnegie Mellon University, Department of Chemistry

Polymer Chemistry

ARTICLE

Transformation of Gels via Catalyst-Free Selective RAFT Photoactivation

Received 00th January 20xx,
Accepted 00th January 20xx

DOI: 10.1039/x0xx00000x

www.rsc.org/

Sivaprakash Shanmugam[a†], Julia Cuthbert[a†], Jacob Fluma, Marco Fantin[a], Cyrille Boyer[b], Tomasz Kowalewski[a], Krzysztof Matyjaszewski[a]*

Abstract: This work explores the concept of structurally tailored and engineered macromolecular (STEM) networks by proposing a novel metal-free approach to prepare the networks. STEM networks are composed of polymer networks with latent initiator sites affording post-synthesis modification. The proposed approach relies on selectively activating the fragmentation of trithiocarbonate RAFT agent by relying on visible light RAFT iniferter photolysis coupled with RAFT addition-fragmentation process. The two-step synthesis explored in this work generates networks that are compositionally and mechanically differentiated than their pristine network. In addition, by careful selection of crosslinkers, conventional poly(ethylene glycol) dimethacrylate (M_n =750) or trithiocarbonate dimethacrylate crosslinker (bis[(2-propionate)ethyl methacrylate] trithiocarbonate (bisPEMAT)), and varying concentrations of RAFT inimer (2-(2-(n-butyltrithiocarbonate)-propionate)ethyl methacrylate (BTPEMA)), three different types of primary (STEM-0) poly(methyl methacrylate) (PMMA) networks were generated under green light irradiation. These networks were then modified with methyl acrylate (MA) or *N,N*-dimethylacrylamide (DMA), under blue light irradiation to yield STEM-1 gels that are either stiffer or softer with different responses to polarity (hydrophilicity/hydrophobicity).

Introduction

Functional materials that are capable of undergoing post-synthetic modification from an initially synthesized primary scaffold have been recently gaining interest.[1-7] In order to achieve this, different techniques in reversible deactivation radical polymerizations (RDRP), including reversible addition-fragmentation chain transfer (RAFT) polymerization,[8] atom transfer radical polymerization (ATRP),[9-11] and nitroxide mediated polymerization (NMP),[12] have been developed and exploited. RDRP techniques allow for unique tailoring of functional polymer networks.[13-15] In addition, a recent interest in photochemistry has led to the application of RDRP techniques to promote external regulation in polymerization, and therefore, enabling synthesis of materials with precise spatial, temporal and sequence control.[16-19]

Johnson and coworkers, for instance, have recently developed a novel concept called Photo-Redox Catalyzed Growth (PRCG) that enabled spatiotemporal control over gel synthesis.[20] In their approach, a "parent" gel was synthesized via click chemistry of 4-arm poly(ethylene glycol) (PEG) star polymer with dibenzocyclooctyne (Tetra-DBCO-PEG) and a bis-azide trithiocarbonate (bis-N_3-TTC) in the presence of monomer and phenothiazine (PTH) photocatalyst and/or crosslinker. RAFT polymerization of acrylates and acrylamides was then carried out by PTH under visible light irradiation, allowing manipulation of polymer chain length, crosslinking density, and composition of polymer network. This led to mechanically and chemically differentiated "daughter" gels. In addition, dual RDRP that relies on the orthogonality of two polymerization techniques has been developed to avoid chemical transformations between polymerization steps.[21] Dual RDRP approaches have been used to generate many polymers with complex architectures including bottlebrush polymers,[22] star polymers,[23] and multiblock copolymers.[24] An important application of the dual RDRP approach is the concept of structurally tailored and engineered macromolecular (STEM) networks.[1]

The STEM networks are versatile materials containing latent functional groups available for post-synthesis modifications to introduce new chemical and material properties. For example, multifunctional hydrogels were synthesized by colloidal crystal templating to create 3D ordered microporous (3DOM) structures.[4] The 3DOM structure could be tailored post-synthesis to introduce hydrophobic or hydrophilic polymers, fluorescent moieties, and conducting polymers. More recently, the STEM networks were prepared by conventional free radical polymerization (FRP) of a (meth)acrylate monomer and

[a] *Department of Chemistry, Carnegie Mellon University, 4400 Fifth Avenue, Pittsburgh, Pennsylvania, 15213, United States.*
[b] *Centre for Advanced Macromolecular Design (CAMD) and Australian Centre for NanoMedicine School of Chemical Engineering, UNSW Australia, Sydney, NSW 2052, Australia.*
† S.S. and J.C. contributed equally.
Electronic Supplementary Information (ESI) available: Experimental details, ^{1}H NMR spectra, ESI-MS spectra, kinetic plots, SEC Traces, rheology temperature ramp results, and swelling ratios. See DOI: 10.1039/x0xx00000x

a photoactive inimer, which could generate radicals when exposed to UV light.[3] The same principle was extended to a dual RDRP approach by synthesizing the primary network by RAFT polymerization and incorporating an ATRP initiator monomer for orthogonal polymeric functionalization.[1]

We previously reported a novel catalyst-free orthogonal polymerization approach that relies on only RAFT polymerization.[25,26] In that work, we explored the use of catalyst-free selective activation to develop STEM gels by simple manipulation of visible light wavelengths, thus simplifying experimental conditions and purification. We now use this two-step approach that utilizes metal-free RAFT photoiniferters to design STEM gels. Unlike previously proposed STEM gel synthesis, this approach does not require dual RDRP chemistries. Rather, only RAFT polymerization using visible light RAFT iniferters is employed. This is a facile setup, using just commercially available narrow visible light LEDs without the need for an external initiator.

In this work, first, a primary or "STEM-0" network was designed by mediating polymerization of methyl methacrylate (MMA) by 4-cyano-4-[(dodecylsulfanylthiocarbonyl)sulfanyl]pentanoic acid (CDTPA) under green light irradiation in the presence of either a conventional or RAFT crosslinker with varying concentrations of inimer. Depending on the crosslinker used and inimer concentration, three different types of STEM-0 gels were synthesized. The three STEM-0 networks could be post-modified in the following methods: i) grafting chains from the STEM-0 network, ii) "expanding" the length of the crosslinker, or iii) a combination of the two above-described methods. The second step involved modification of STEM-0 networks to form STEM-1 networks by using either methyl acrylate (MA) or *N,N*-dimethyl acrylamide (DMA) under high intensity blue light irradiation. The addition of MA or DMA units into the gel was aimed to either soften or stiffen the gels, respectively, and consequently, generate STEM-1 networks with varying mechanical properties in comparison to their original STEM-0 counterparts.

Results and Discussion

Catalyst-free Selective RAFT Polymerization Photoactivation

In our previous investigation, a novel concept of catalyst-free selective activation was developed for synthesis of well-defined bottlebrush and comb-like copolymers.[25] Selective activation was achieved by careful selection of RAFT agents with desired R and Z groups, and through manipulation of visible light wavelengths. This approach allowed for the initial activation of 4-cyano-4-[(dodecylsulfanylthiocarbonyl)sulfanyl]pentanoic acid (CDTPA) by generating tertiary carbon radicals through photolysis of R-groups under green light irradiation promoting polymerization of methacrylates. In addition, RAFT agents with R-groups composed of secondary carbon radical leaving groups remained inert under green light irradiation and did not participate in chain transfer reactions with tertiary carbon radicals. This concept was employed to incorporate RAFT inimers (BTPEMA) with secondary carbon radical leaving groups that can be activated under blue light irradiation to polymerize acrylates/acrylamides leading to complex architectures such as bottlebrushes. In this work, catalyst-free selective activation was employed for generation of different STEM gels through careful selection of crosslinkers and inimers (Scheme 1).

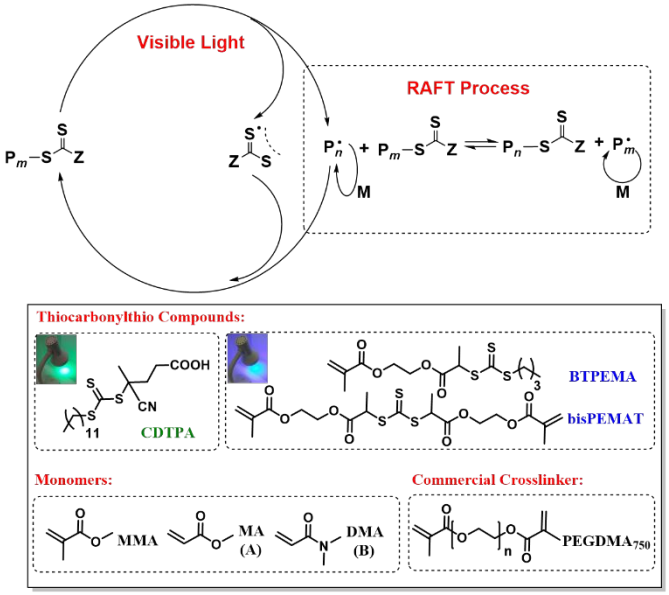

Scheme 1. RAFT photoiniferter approach employed for the synthesis of STEM gels using various trithiocarbonates, monomers, and crosslinkers: 4-cyano-4-[(dodecylsulfanylthiocarbonyl)sulfanyl]pentanoic acid (CDTPA), 2-(2-(n-butyltrithiocarbonate)-propionate)ethyl methacrylate (BTPEMA) bis[(2-propionate)ethyl methacrylate] trithiocarbonate (bisPEMAT), methyl methacrylate (MMA), methyl acrylate (MA, A), N,N-dimethyl acrylamide (DMA, B), and poly(ethylene glycol) dimethacrylate (Molar mass, M_w = 750 g/mol).

Catalyst-free selective RAFT Photoactivation for STEM Gels Synthesis

Catalyst-free selective RAFT photoactivation for STEM gel synthesis involves photolysis of RAFT agents under the visible light wavelengths via spin-forbidden n → π* electronic transition that enables β-scission of the C-S bond (Scheme 1). Under green light irradiation in the presence of CDTPA, STEM-0 networks composed of crosslinked PMMA were generated (Scheme 2, Table 1). In this approach, three different STEM-0 networks and several different types of STEM-1 networks were generated by varying a RAFT inimer and RAFT crosslinker (Scheme 1, Table 1). The first type, referred to as the dangling or "D-STEM-0" network was made up of PMMA crosslinked with $PEGDMA_{750}$ with incorporation of BTPEMA (one RAFT R group) in the first step for the sequent polymerization of dangling side chains (Scheme 2A, Table 1). The second type was the expandable or "E-STEM-0" network was made by

crosslinking PMMA with bisPEMAT (two RAFT R groups) without BTPEMA or $PEGDMA_{750}$ (Scheme 2B, Table 1). The third "D/E-STEM-0" network was composed of both BTPEMA and bisPEMAT (Scheme 2C, Table 1), thus allowing for both polymerization of side chains and expansion of the network. In all types of STEM-0 gels, the second step involved modification of the STEM-0 network under blue light irradiation after infiltrating a second monomer, either MA (A monomer) or DMA (B monomer), to generate STEM-1A or STEM-1B gels, respectively (Scheme 2).

In the case of D-STEM-1 networks, the second monomer grows from both the side RAFT agents (BTPEMA) and from the chain end (CDTPA) of the D-STEM-0 networks. However, this does not change the architecture of the obtained D-STEM-1 networks: the chain growing from the chain end is indistinguishable from the chains growing from the side BTPEMA units. This is analogous to the polymer brush architecture previously reported.[25]

In the case of the E-STEM networks, the second monomer is incorporated in both the cross-linker bisPEMAT and at the chain end (CDTPA). Twice as much monomer is incorporated in each cross-linked unit because of its symmetrical nature (polymer chains grow from both sides of the trithiocarbonate unit of bisPEMAT). A block copolymer is effectively made with the original network chains after extension of the terminal CDTPA.

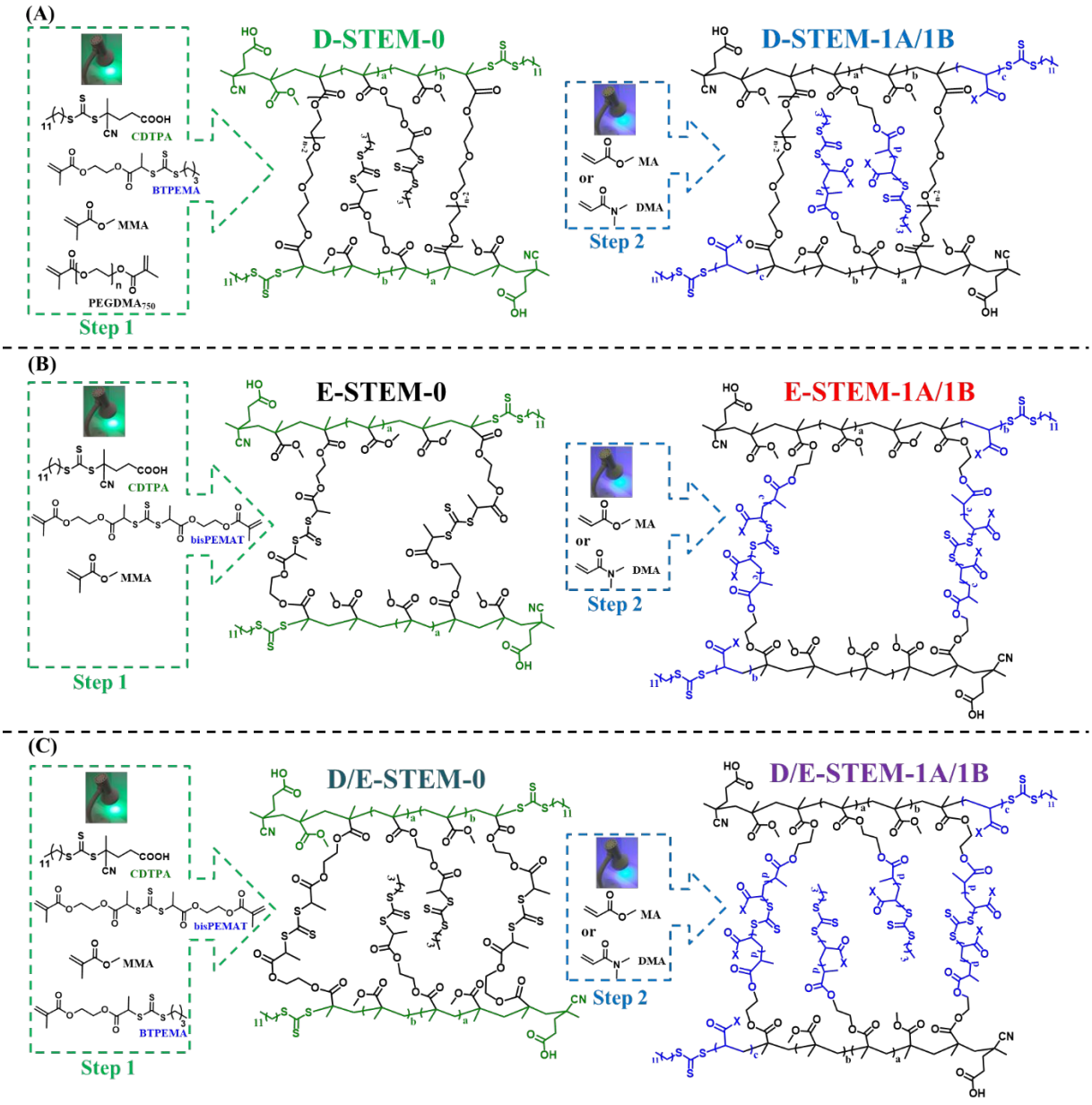

Scheme 2. Synthesis of various types of PMMA STEM-0 networks (A-C, Step 1) under green light irradiation followed by post-modification under blue light to yield STEM-1A/1B networks (A-C, Step 2) incorporating PMA or PDMA (X represents either -OCH_3 or -$N(CH_3)_2$). (A) D (Dangling BTPEMA)-STEM-0 PMMA network crosslinked by $PEGDMA_{750}$ in the presence of BTPEMA before modification to yield D-STEM-1A or 1B network; (B) E(Expandable bisPEMAT crosslinker)-STEM-0 PMMA network crosslinked by bisPEMAT before modification to yield E-STEM-1A or 1B network; and (C) D/E- (Dangling and Expandable) STEM-0 PMMA network crosslinked by bisPEMAT in the presence of BTPEMA before modification to yield D/E-STEM-1A or 1B network. Note that RAFT is a statistical polymerization. Therefore, the proposed gel structures are idealized.

Table 1. A summary of the STEM-0 and STEM-1 gels synthesized and the results of post-synthesis modifications.

Entry	Type of STEM Gel[1]	MMA:CDTPA:X:BTPEMA:M_2[2,3]	Crosslinker	Conv. M_2	M_2 (avg 2nd monomer units per RAFT R group)[4]	Tan (δ) Maxima (°C)[5]
1	D-STEM-0 dense	200:1:2:20:0	$PEGMA_{750}$			28, 74
2	D-STEM-1A dense	200:1:2:20:50	$PEGMA_{750}$	18%	MA (9)	41
3	D-STEM-1B dense	200:1:2:20:50	$PEGMA_{750}$	30%	DMA (15)	85
4	D-STEM-0 mid	200:1:2:10:0	$PEGMA_{750}$			42,75
5	D-STEM-1A mid	200:1:2:10:50	$PEGMA_{750}$	26%	MA (13)	45
6	D-STEM-0 sparse	200:1:2:5:0	$PEGMA_{750}$			74
7	D-STEM-1A sparse	200:1:2:5:50	$PEGMA_{750}$	36%	MA (18)	59
8	E-STEM-0	200:1:2: 0:0	bisPEMAT			70, 126
9	E-STEM-1A	200:1:2:0:200	bisPEMAT	38%	MA (45)	84
10	E-STEM-1B	200:1:2:0:200	bisPEMAT	65%	DMA (79)	90, 120
11	D/E-STEM-0	200:1:2:20:0	bisPEMAT			37, 86
12	D/E-STEM-1A	200:1:2:20:25	bisPEMAT	36%	MA (8)	41, 78
13	D/E-STEM-1B	200:1:2:20:33	bisPEMAT	39%	DMA (12)	88

[1]Dense, mid, and sparse refer to the theoretical grafting density of dangling polymer side chains, which is determined by the ratio of CDTPA:BTPEMA.[2]X = crosslinker. [3]See the supporting information for experimental details. [4] The 2nd monomer (either MA or DMA) infiltrated into the STEM-0 network for post-synthesis grafting from to produce the STEM-1 networks. [5]Determined from dynamic mechanical analysis temperature ramps. The T_g was taken as the temperature at the tan (δ) local maxima.

Linear Model Systems

Before synthesizing the PMMA networks, a linear model for the copolymerization of MMA with BTPEMA without any crosslinkers was prepared. Kinetic studies on different concentrations of BTPEMA ([CDTPA]:[BTPEMA] = 1:0, 1:5, 1:10, 1:20) were carried out under green light irradiation (λ_{max} = 520 nm, intensity = 4.25 mW/cm^2) (Supporting Information, Figure S3).[26] It is important that the chain-transfer group in BTPEMA remains unaffected under these polymerization conditions, to allow its use as a chemical handle for further modifications. The different concentrations of BTPEMA led to pseudo-first-order kinetics with the apparent propagation rate constants (k_p^{app}) (Figure S3A) decreasing with increasing BTPEMA concentrations (k_p^{app} = 9.25 × 10^{-3} min^{-1}, 9.21 × 10^{-3} min^{-1}, 7.05 × 10^{-3} min^{-1}, and 6.46 × 10^{-3} min^{-1} for [CDTPA]:[BTPEMA] of 1:0, 1:5, 1:10, and 1:20, respectively). This decrease in polymerization rate can be attributed to the presence of an additional reaction pathway that reduces radical concentration proposed in our previous investigation.[25] This reduction of radical concentration was clearly seen with increasing concentrations of BTPEMA leading to slower polymerization as well as increased length of inhibition periods ([CDTPA]:[BTPEMA] of 1:0, 1:5, 1:10, and 1:20 have inhibition periods of 22 min, 35 min, 45 min, and 60 min, respectively). Most importantly, the reactions with different concentrations of BTPEMA reached high monomer conversions (≥ 90%) (Table S1) in 4 to 6 hours. NMR analysis (Figures S5-S8) revealed that the trithiocarbonate pendant groups on BTPEMA, primarily the peak at 4.8 ppm which corresponds to the -CH of BTPEMA adjacent to the trithiocarbonate, remained intact even at high MMA conversions. In addition, analysis of GPC traces upon increasing BTPEMA concentrations showed a monomodal distribution of polymer chains with narrow molecular weight distributions (Figures S3B, S3C & S4).

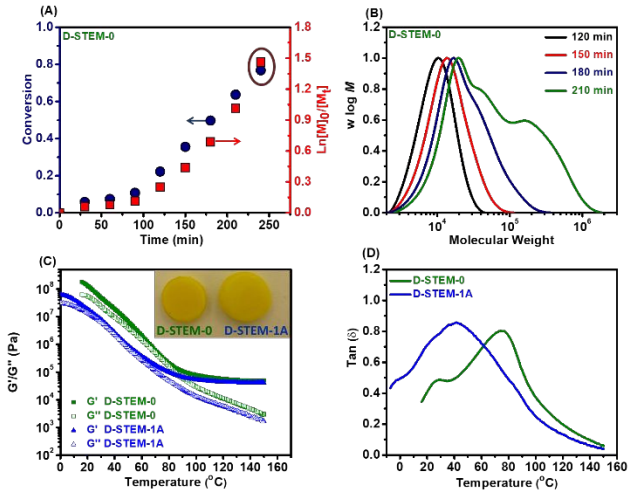

Figure 1. D-STEM-0 network synthesis under green light irradiation (λ_{max} = 520 nm, intensity = 4.25 mW/cm^2) with [MMA]:[CDTPA]:[PEGDMA$_{750}$]:[BTPEMA] of 200 : 1 : 2 : 20, 50% v/v monomer concentration, followed by further modification with MA under blue light irradiation (λ_{max} = 465 nm, intensity = 6.5 mW/cm^2) to give the D-STEM-1A network. (A) Plots of conversion and Ln([M$_0$]/[M]$_t$) vs. exposure time with brown circle representing monomer conversion upon reaching gelation point; (B) GPC traces mapping the studies of gelation of PMMA for the preparation of D-STEM-0; (C) Temperature dependence on the storage (G') and loss moduli (G"); and (D) tan(δ) of D-STEM-0 network composed of PMMA$_{200}$-*rand*-P(BTPEMA)$_{20}$ and of D-STEM-1A network composed of PMMA$_{200}$-*rand*-P(BTPEMA-*graft*-PMA$_9$)$_{20}$-*block*-PMA$_9$.

STEM Gels Synthesis and Characterization

In order to understand the formation of crosslinked PMMA networks via the RAFT photoiniferter approach, kinetic experiments for D-STEM-0 with PEGDMA$_{750}$ crosslinkers were carried out with different concentrations of BTPEMA (Figures 1 & S9 and Table S2). The k_p^{app} for the different concentrations of BTPEMA relative to CDTPA ([BTPEMA]:[CDTPA]) 1:0, 1:5, 1:10, and 1:20 were determined to be 1.26 × 10^{-2} min^{-1}, 9.38 × 10^{-3} min^{-1}, 7.81 × 10^{-3} min^{-1}, and 5.7 × 10^{-3} min^{-1}, respectively. The polymerization rates for the linear model and the crosslinked PMMA network in the presence of different concentrations of BTPEMA were found to be quite similar. In addition, the gelation point (represented by the brown circle in Figure 1A and determined visually as the time at which the gel did not flow upon inverting the vial) was reached at high monomer conversions (≥ 80%) in a period of 2.5 to 4 hours for the different concentrations of BTPEMA (Table S2). During network formation, the GPC traces revealed increase in molecular weight due to growth of individual polymer chains and the crosslinking between polymer chains; crosslinking also broadened the molecular weight distributions (Figures 1B & S9). The synthesis of D-STEM-0 network was then repeated using the formulation highlighted in Figure 1 with [CDTPA]:[BTPEMA] of 1:20 with irradiation time of 12 hours to ensure complete MMA conversion. The synthesized gel was then dried in a vacuum oven at 50˚C for a week to remove solvent and unreacted MMA. Next, the gel was infused with MA through overnight swelling. The gel was then placed under blue light irradiation (λ_{max} = 465 nm, intensity = 6.5 mW/cm^2; light intensity that is 10 times higher compared to a typical photocatalyst mediated polymerization[27,28]) to promote polymerization of MA. Gravimetric analysis revealed that, on average, 9 units of MA were added to each trithiocarbonate to generate D-STEM-1A gel. The modified gel was dried in a vacuum oven at 50˚C for a week to remove monomer and solvent.

Dynamic mechanical analysis was then carried out on D-STEM-0 and D-STEM-1A gels in their dried state by monitoring the storage (G') and loss (G") moduli and the damping factor, tan(δ) (tan(δ) = G"/ G') during temperature sweeps. From 20˚C to 100˚C, both D-STEM-0 and STEM 1A gels passed through their glass transition temperature (T$_g$, represented by the local maximum on the tan(δ) curve) and arrived at a soft, rubbery plateau (Figure 1C). For the D-STEM-0 gel, the two local maxima observed in the tan(δ) curve most probably resulted from phase separation of the PMMA chains from BTPEMA-rich regions in the network, due to unfavorable interaction between PMMA and BTPEMA. The first local maximum at 74˚C can be attributed to the T$_g$ of the main PMMA network while the second local maximum at 28˚C can be attributed to the T$_g$ of BTPEMA-rich regions. However, upon grafting MA from the BTPEMA units, not only did the T$_g$ of the D-STEM-1A gel decrease to 41˚C, but also displayed only a single tan(δ) maximum value (Figure 1D), suggesting that the side chains were miscible with the PMMA network. D-STEM-0 networks prepared with [CDTPA]:[BTPEMA] of 1:10, thus with less dense side-chain inimers, also displayed the same two local maxima in the tan(δ) curve (Figure S10 B&D). Grafting of MA from this network to generate a softer (lower T$_g$ material) D-STEM-1A network led to the addition of 13 units of MA per inimer. This network, after modification with PMA grafting, displayed a single tan(δ) maximum value of 45˚C. Further lowering of [CDTPA]:[BTPEMA] to 1:5 substantially diminished the effects of phase separation observed between PMMA and PBTPEMA due to low content of BPTEMA (Figure S10 A&B).

In order to show that this approach is viable for the synthesis of stiffer (higher T$_g$ material) networks from D-STEM-0, DMA side chains (15 units) were grown from each inimer. This resulted in stiffer network (D-STEM-1B, Figure S11), in which a single tan(δ) maximum (85˚C) was observed. In addition, introducing hydrophilic DMA chains to PMMA STEM-0 networks enabled swelling in both water and DMSO (Figure S12).

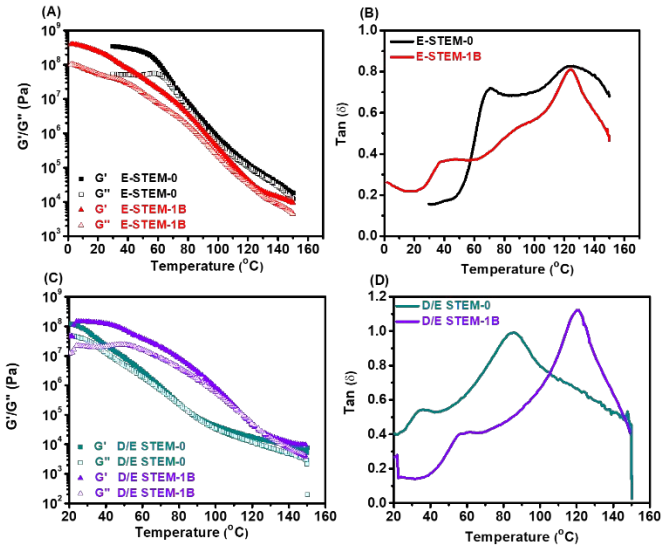

Figure 2. E- and D/E-STEM-0 networks synthesized under green light irradiation (λ_{max} = 520 nm, intensity = 4.25 mW/cm^2) followed by further modification with DMA under blue light irradiation (λ_{max} = 465 nm, intensity = 6.5 mW/cm^2) to give E-STEM and D/E-STEM-1B. (A,B) Temperature dependence on the storage (G') and loss moduli (G") and tan(δ) of E-STEM-0 network composed of $PMMA_{200}$-*rand*-$P(bisPEMAT)_2$ and of E-STEM-1B network composed of $PMMA_{200}$-*rand*-P(bisPEMAT-*block*-$PDMA_{158})_2$-block-$PDMA_{79}$; (C,D) Temperature dependence on the storage (G') and loss moduli (G") and tan(δ) of D/E-STEM-0 network composed of $PMMA_{200}$-*rand*-$P(bisPEMAT)_2$-*rand*-$P(BTPEMA)_{20}$ and of D/E-STEM-1B network composed of $PMMA_{200}$-*rand*-P(bisPEMAT-*block*-$PDMA_{24})_2$-*rand*-P(BTPEMA-*graft*-$PDMA_{12})_{20}$-*block*-$PDMA_{12}$.

For the E- and D/E-STEM-0 networks, crosslinking of PMMA was carried out with bisPEMAT. Kinetic experiments for E- and D/E-STEM-0 networks (Figure S13 and Table S3) with bisPEMAT and different concentrations of BTPEMA revealed a similar trend with $PEGDMA_{750}$ crosslinker where the k_p^{app} decreased with increasing concentrations of BTPEMA due to the formation of long-lived adduct radicals: [BTPEMA]:[CDTPA] of 1:0, 1:10, and 1:20 led to k_p^{app} of 1.46 × 10^{-2} min^{-1}, 1.25 × 10^{-2} min^{-1}, and 1.19 × 10^{-2} min^{-1}, respectively. Gelation points (Figure S13A-C) were reached at high monomer conversions (≥ 90%) in a period of 3 to 4.5 hours (Table S3) for the different concentrations of BTPEMA. Like for networks synthesized with $PEGDMA_{750}$, increase in molecular weight with conversion and broadening of molecular weight distributions were observed (Figure S13D-F) with bisPEMAT.

Except for the formulations, the synthetic steps of E- and D/E-STEM-0 networks were similar to the D- STEM-0 network. Both E- and D/E-STEM-0 networks were then infused with either MA or DMA monomers for grafting of side chains and blocks into the networks to generate E- and D/E- STEM-1A/1B networks Figure 2A-D). When MA was incorporated into the networks, it had the effect of softening the materials (decreased the T_g) (Table 1, Figure S15A-D). Incorporation of DMA as a block copolymer to synthesize E-STEM-1B network led to the addition of 131 monomer units into each trithiocarbonate, with significant expansion of the network (Figure 2C&D). Likewise, incorporation of DMA as a block copolymer and side chain to synthesize D/E-STEM-1B network led to the addition of 13 monomer units into each trithiocarbonate, thus with a lower expansion of the network, but a significant incorporation of PDMA side chains. Shorter chains were added to D/E- and D-STEM networks because of the larger amount of BTPEMA units in these networks.

Dynamic mechanical analysis revealed that addition of DMA as a block changed the tan(δ) profile in comparison to E-STEM-0 network (Figure 2A&B). The E-STEM-1B network tan (δ) measurement revealed a sharper local maximum at 120˚C corresponding the T_g of PMMA and a shoulder around 90˚C corresponding to the T_g of PDMA (Figure 2D). This was not observed in the D-STEM-1B network (Figure S11B), suggesting the network macromolecular architecture was different between the RAFT inimer and crosslinker networks. The presence of PDMA blocks in the E-STEM-1B network enabled swelling in water (Figure S14).

The presence of PDMA side chains in the D/E-STEM-1B network led to a significant increase in the T_g in comparison to D/E-STEM-0 network (Figure 2C). The local maximum at 86˚C can be attributed to the T_g of PMMA network plasticised by the RAFT inimer (see similar tan (δ) profile of D-STEM-0, in comparison to that of E-STEM-0). The second local maximum at 37˚C can be attributed to the T_g of PBTPEMA. Upon grafting of DMA from PBTPEMA, the D/E-STEM-1B gel displayed a sharp tan(δ) maximum value at 120˚C, corresponding the T_g of PMMA, but without the shoulder observed in the E-STEM-1B gel. The D/E-STEM gels displayed similar swelling properties as the E-STEM gels (Figure S14).

Conclusions

This work demonstrated a novel approach in designing STEM gels by employing a chemoselective visible light RAFT polymerization that can be employed without the presence of photocatalysts. This approach was divided into two steps. First, a primary network, namely STEM-0, was synthesized with CDTPA as green light iniferter in the presence of MMA, crosslinker ($PEGDMA_{750}$ or bisPEMAT), and BTPEMA. In the second step the primary network is modified under blue light irradiation in the presence of DMA or MA to generate side chains and block copolymers. Furthermore, this approach allowed for a stiff PMMA primary network (STEM-0) to be modified to become a softer or stiffer (STEM-1) network depending on the use of either MA or DMA. Dynamic mechanical analysis was used to characterize the moduli of the starting and end materials, and also to determine their glass transition temperatures.

Conflicts of interest

There are no conflicts to declare.

Acknowledgements

We thank the NSF DMR 1436219 and 1436201 and DoE ER 45998 for financial support. We thank Dr. Roberto Gil and the NMR facility at CMU was partially supported by NSF grants CHE-9808188, CHE-1039870 and CHE-1726525.

Notes and references

1 J. Cuthbert, A. Beziau, E. Gottlieb, L. Fu, R. Yuan, A. C. Balazs, T. Kowalewski and K. Matyjaszewski, Macromolecules, 2018, 51, 3808-3817.
2 H. Sun, C. P. Kabb, Y. Dai, M. R. Hill, I. Ghiviriga, A. P. Bapat and B. S. Sumerlin, Nature Chemistry, 2017, 9, 817.
3 A. Beziau, A. Fortney, L. Y. Fu, C. Nishiura, H. B. Wang, J. Cuthbert, E. Gottlieb, A. C. Balazs, T. Kowalewski and K. Matyjaszewski, Polymer, 2017, 126, 224-230.
4 H. He, S. Averick, P. Mandal, H. Ding, S. Li, J. Gelb, N. Kotwal, A. Merkle, S. Litster and K. Matyjaszewski, Advanced Science, 2015, 2, 1500069.
5 R. F. Pereira, A. Sousa, C. C. Barrias, P. J. Bártolo and P. L. Granja, Materials Horizons, 2018, DOI: 10.1039/C8MH00525G.
6 A. Mpoukouvalas, W. Li, R. Graf, K. Koynov and K. Matyjaszewski, ACS Macro Letters, 2013, 2, 23-26.
7 K. Matsukawa, T. Masuda, A. M. Akimoto and R. Yoshida, Chem Commun (Camb), 2016, 52, 11064-11067.
8 C. Boyer, V. Bulmus, T. P. Davis, V. Ladmiral, J. Liu and S. Perrier, Chemical Reviews, 2009, 109, 5402-5436.
9 A. Anastasaki, V. Nikolaou, G. Nurumbetov, P. Wilson, K. Kempe, J. F. Quinn, T. P. Davis, M. R. Whittaker and D. M. Haddleton, Chemical Reviews, 2016, 116, 835-877.
10 K. Matyjaszewski and N. V. Tsarevsky, Journal of the American Chemical Society, 2014, 136, 6513-6533.
11 N. V. Tsarevsky and K. Matyjaszewski, Chemical Reviews, 2007, 107, 2270-2299.
12 C. J. Hawker, A. W. Bosman and E. Harth, Chemical Reviews, 2001, 101, 3661-3688.
13 C. Tsitsilianis, G. Serras, C. Ko, F. Jung, C. Papadakis, M. Rikkou-Kalourkoti, C. S. Patrickios, R. Schweins, and C. Chassenieux, Macromolecules, 2018, 51, 2169-2179.
14 P. Chakma, Z. Digby, J. Via, M.P. Schulman, J.L. Sparks, and D. Konkoewicz, Polymer Chemistry, 2018, 9, 4744-4756.
15 R. Tamate, T. Ueki, Y. Kitazawa, M. Kuzunuki, M. Watanabe, A.M. Akimoto, and R. Yoshida, Chemistry of Materials, 2016, 28, 6401-6408.
16 S. Shanmugam, J. Xu and C. Boyer, Macromolecular Rapid Communications, 2017, 38, 1700143.
17 X. Pan, M. Fantin, F. Yuan and K. Matyjaszewski, Chemical Society Reviews, 2018, 47, 5457-5490.
18 E. H. Discekici, A. Anastasaki, J. Read de Alaniz and C. J. Hawker, Macromolecules, 2018, 51, 7421-7434.
19 X. Pan, M. A. Tasdelen, J. Laun, T. Junkers, Y. Yagci and K. Matyjaszewski, Progress in Polymer Science, 2016, 62, 73-125.
20 M. Chen, Y. Gu, A. Singh, M. Zhong, A. M. Jordan, S. Biswas, L. T. J. Korley, A. C. Balazs and J. A. Johnson, ACS Central Science, 2017, 3, 124-134.
21 S. Pearson, C. St Thomas, R. Guerrero-Santos and F. D'Agosto, Polymer Chemistry, 2017, 8, 4916-4946.
22 R. Fenyves, M. Schmutz, I. J. Horner, F. V. Bright and J. Rzayev, Journal of the American Chemical Society, 2014, 136, 7762-7770.
23 K. Ranganathan, R. Deng, R. K. Kainthan, C. Wu, D. E. Brooks and J. N. Kizhakkedathu, Macromolecules, 2008, 41, 4226-4234.
24 J. C. Theriot, G. M. Miyake and C. A. Boyer, ACS Macro Letters, 2018, 7, 662-666.
25 S. Shanmugam, J. Cuthbert, T. Kowalewski, C. Boyer and K. Matyjaszewski, Macromolecules, 2018, 51, 7776-7784.
26 J. Xu, S. Shanmugam, N. A. Corrigan and C. Boyer, in Controlled Radical Polymerization: Mechanisms, American Chemical Society, 2015, vol. 1187, ch. 13, pp. 247-267.
27 J. Xu, K. Jung, A. Atme, S. Shanmugam and C. Boyer, Journal of the American Chemical Society, 2014, 136, 5508-5519.
28 J.R. Lamb, K.P. Qin and J.A. Johnson, Polymer Chemistry, 2019, 10, 1585-1590.

TOC